

Investigation on FTIR spectra of barium calcium titanate ceramics

Xueqin Jin · Dazhi Sun · Mingjun Zhang · Yudan Zhu · Juanjuan Qian

Received: 31 August 2007 / Accepted: 16 December 2007 / Published online: 3 January 2008
© Springer Science + Business Media, LLC 2007

Abstract Barium titanate, which is applied in many fields, is a kind of very important ferroelectric material because it is lead free. Its physical properties are changed by replacement or addition of other ions. Here, barium calcium titanate ((Ba,Ca)TiO₃) ceramics are prepared. The concentration of calcium is up to 20 at.%. The Fourier transformation infrared spectroscopy (FTIR) measurement is carried out in order to reveal the vibration of crystal lattices. The influence of the replacement on the interaction between Ti and O can be observed by investigating the absorption peak of the Ti–O bond. The wavenumber of absorption peak of Ti–O bond becomes larger with increase of the content of Ca, even though the concentration of Ti is not changed. The wavenumber of absorption peak in (Ba_{0.95}Ca_{0.05})TiO₃ is near 525 cm⁻¹ while that in (Ba_{0.80}Ca_{0.20})TiO₃ is near 550 cm⁻¹. It is attributed to the decrease of the cell size. The length of Ti–O bond is shortened by replacement of Ca. Then the interaction between Ti and O is enhanced. The similar phenomenon is observed in (Ba,Mg)TiO₃ and alkali doped BaTiO₃ materials as well, supporting the mechanism. Furthermore, the aging effect in (Ba,Ca)TiO₃ and (Ba,Mg)TiO₃ systems is observed. The former exhibits a good stability when the latter shows unstable FTIR spectra. The influence of point defects on the aging effect is discussed. These results indicate that the FTIR measurement is helpful to study the relationship between the structure and physical properties of ferroelectric materials.

Keywords Doped barium titanate · Barium calcium titanate · FTIR · Aging · Point defect

1 Introduction

Ferroelectric materials are widely applied in many fields, such as IT, energy conversion and infrared detection [1] because they possess excellent piezoelectric, dielectric and pyroelectric performances [2, 3]. Physical properties in ferroelectric materials are associated with defects [4], additives (or replacements), electric dipoles, crystal structures, ferroelectric domains and so on [5]. The correlation between them has been widely discussed [6–8]. Among them, additives modify the microscopic structure of the material and result in the change of physical properties. Therefore, they play an important role in improvement of performances [5, 9, 10]. According to the soft model theorem, ferroelectricity in perovskite ferroelectric materials depends on the vibration of crystal lattices. Fourier transformation infrared spectroscopy (FTIR) is an effective technique to monitor the reaction process of preparation of materials because it is sensitive to chemical bonds [11, 12]. It can be used to characterize functional materials as well [13, 14]. The information on interaction forces in crystal lattices can be received by Fourier transformation infrared spectroscopy. In the infrared absorption spectra, the position of the absorption peak is determined by the energy of molecule vibration. The higher the energy is, the larger the wavenumber is.

In this paper, a typical ferroelectric material, BaTiO₃ is selected to explore the relationship between additives and FTIR because it possesses a simple perovskite structure. The cell size, crystal structure and binding energy will change when ions are doped in the system, resulting in

X. Jin · D. Sun (✉) · M. Zhang · Y. Zhu · J. Qian
Department of Chemistry,
Shanghai Normal University, 100 Guilin Road,
Shanghai 200234, China
e-mail: sundazhi@shnu.edu.cn

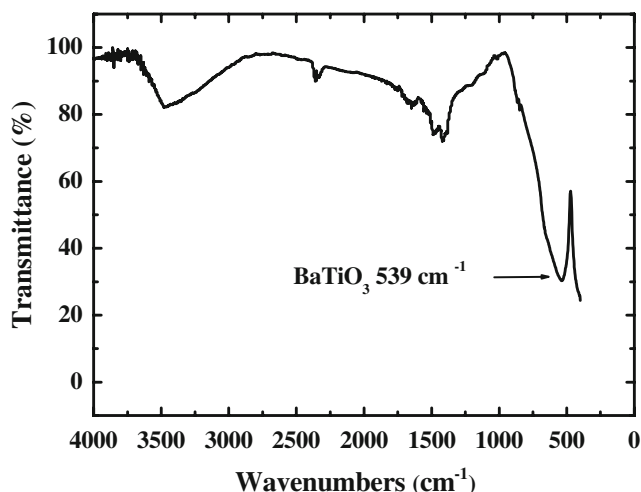


Fig. 1 FTIR spectrum of pure barium titanate material

spectral variation. Here, we report the spectra of FTIR in ferroelectric (Ba,Ca)TiO₃, barium titanate doped with calcium. The wavenumber of the absorption peak shifts to a larger value when the concentration of Ca increases. It is attributed to the increase of binding energy resulted from the decrease of cell size. Furthermore, the similar phenomenon is observed in Mg-doped BaTiO₃ materials. The result supports the mechanism as well. These experimental results show that the additives indeed affect the vibration of crystal lattices. When BaTiO₃ is doped with hetero-valence ions, e.g., Li⁺, Na⁺, and K⁺, the situation becomes complex. The results show that effects of different additives are different even though all of these ions belong to alkali. The BaTiO₃ ceramics doped with K⁺ makes the absorption peak shift to a higher frequency, following the law mentioned above. But, the sample doped with the other two ions, respectively, decreases the wavenumber of the

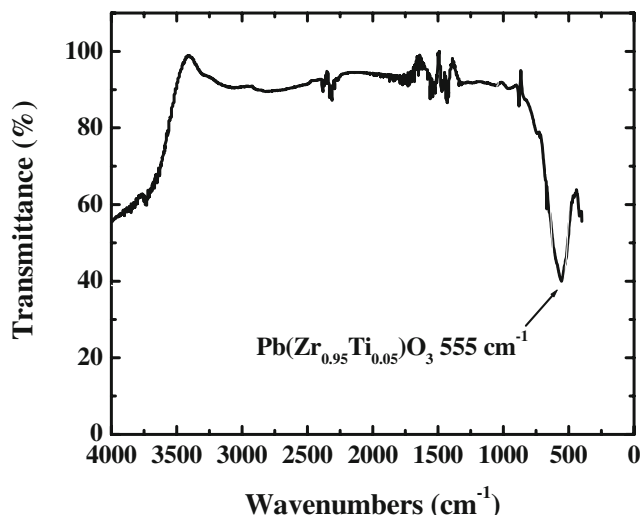
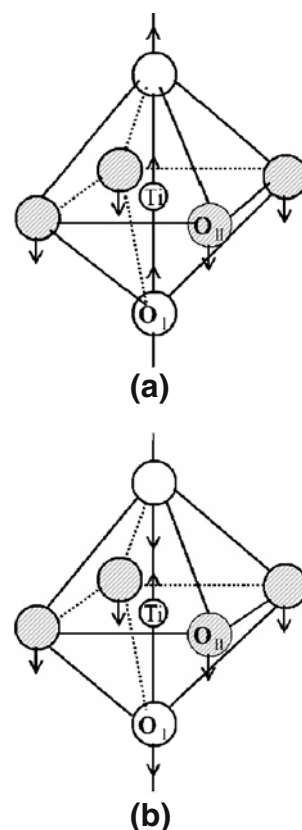


Fig. 2 FTIR spectrum of Pb(Zr_{0.95}Ti_{0.05})O₃ material

Fig. 3 Vibration mode of Ti–O bond: (a) bending vibration, (b) stretching vibration



absorption peak. The strange phenomenon is discussed in terms of the distortion of the TiO₆ octahedron. The aging effect of the FTIR spectra in (Ba,Ca)TiO₃ and (Ba,Mg)TiO₃ is observed as well. No significant change is found in (Ba,Ca)TiO₃, indicating the material is stable. An obvious change is revealed in (Ba,Mg)TiO₃. The mechanism is discussed in terms of the movement of point defects in the system. The Fourier transformation infrared spectroscopy (FTIR) provides an effective method to study the relationship between physical properties and microstructures in ferroelectric materials.

2 Experimental procedures

(Ba,Ca)TiO₃ and (Ba,Mg)TiO₃ materials can be prepared by many kinds of methods, such as solid state reaction [15]. Here, a conventional ceramic process is used to prepare doped BaTiO₃ ceramic samples. The chemical formulas of the materials are (Ba_{1-x}Ca_x)TiO₃, (Ba_{1-y}Mg_y)TiO₃, (Ba_{0.99}Li_{0.01})TiO₃, (Ba_{0.99}Na_{0.01})TiO₃, and (Ba_{0.99}K_{0.01})TiO₃, respectively. Here, $x=0, 0.05, 0.10, 0.15,$ and 0.20 ; $y=0.10, 0.20, 0.30,$ and 0.40 . In alkali doped samples, the amount of dopant is small in order to avoid emergence of other structures because the chemical valence is different. Following ball-milling for 6 h, the mixed raw powder was calcined at 1000°C for 5 h. Then, the powder was ball-

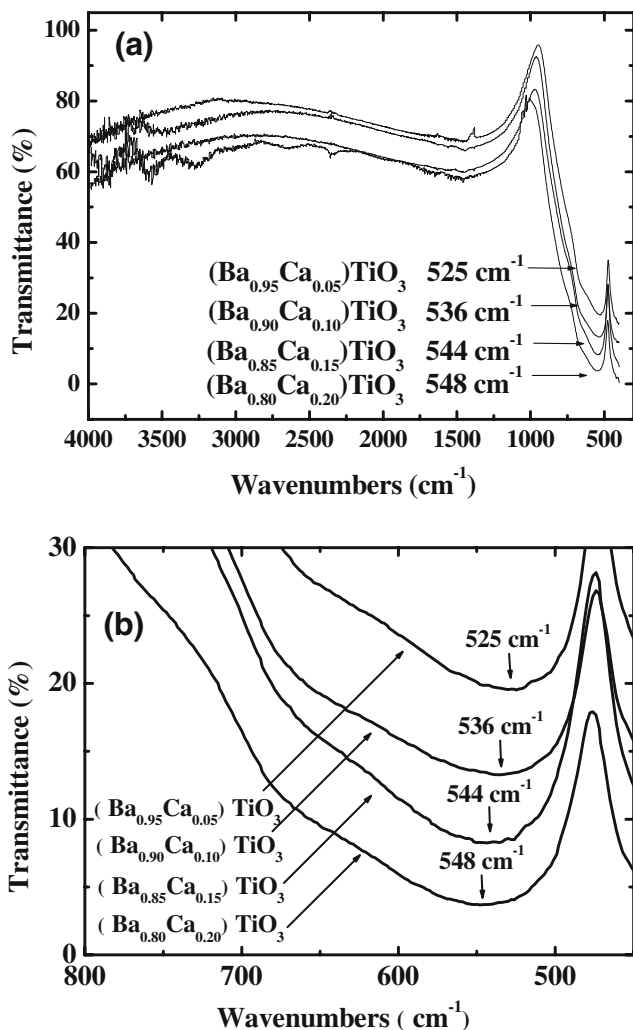


Fig. 4 (a) FTIR spectra of (Ba,Ca)TiO₃ materials. (b) Magnified diagram of absorption peak (the vertical position of some curve is adjusted to avoid overlap of curves)

milled for 8 h. The milled powder was used to form tablets. Finally, the tablets were sintered in air atmosphere at 1350°C for 4 h. The XRD measurement was carried out to determine if the perovskite structure was formed. Transmittance spectra of FTIR were measured to characterize the vibration of crystal lattices. The measurement of FTIR spectrum was carried out by means of Nicolet Avator 370DTGS. The region of wavenumber is from 400 to 4,000 cm^{-1} in the measurement. The main absorption peaks appear below 1,500 cm^{-1} . The peaks are sharp so that the relationship between wavenumbers and chemical compositions can be established clearly. Aging was carried out as the following sequence: (1) Heat the sample through its curie temperature (about 130°C) to 150°C; (2) keep the sample at 150°C for several minutes; (3) cool the sample to 50°C and keep it at the temperature for different periods of time. After aging, the FTIR spectrum was measured instantly at room temperature.

3 Results and discussion

The FTIR spectrum of the pure BaTiO₃ ceramics is shown in Fig. 1. A strong absorption peak appears near 540 cm^{-1} . This peak characterizes the vibration of Ti–O bond, according to the previous research about the titanate [16]. The FTIR spectrum of lead zirconate titanate (see Fig. 2) was measured in order to verify the deduction. In Fig. 2, a strong absorption peak is observed near 550 cm^{-1} . Because oxygen octahedrons in these two systems are very similar, even though some ions are different, the absorption peak in the vicinity of 540 cm^{-1} is assigned to the vibration of O–M (M=ion at B-site) bond. On the other hand, the vibration of Ti–O bond is complex. Besides the observed absorption frequency, there are other two absorption bands [16, 17]. A low frequency band (below 400 cm^{-1}) is assigned to cation-TiO₆ vibration. Another frequency band near 400 cm^{-1} is assigned to the Ti–O_{II} “bending” normal vibration [Fig. 3(a)]. Neither of them is discussed here because the

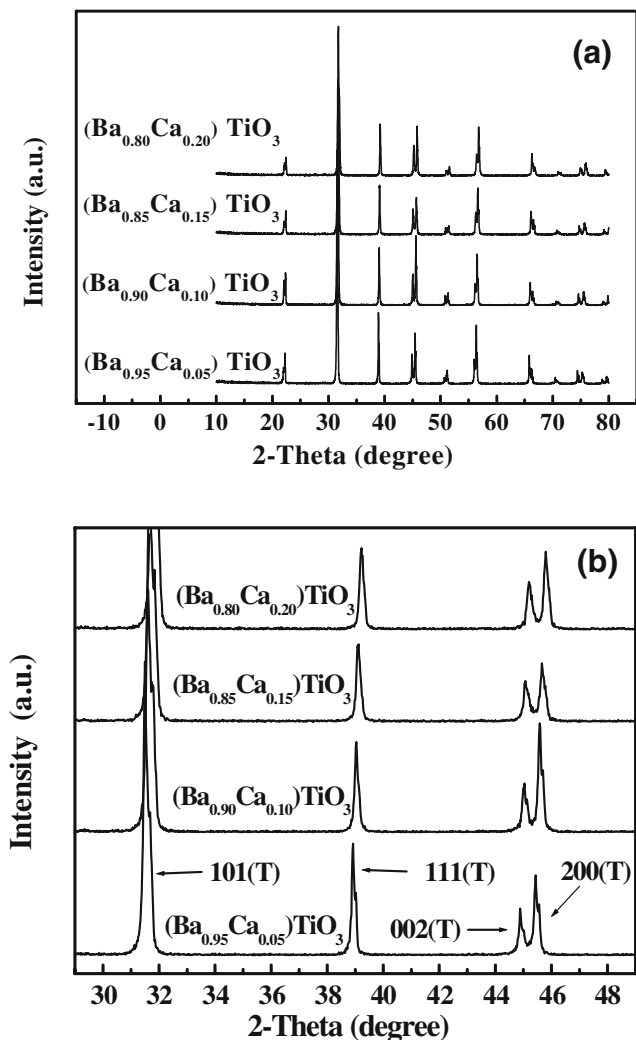


Fig. 5 (a) XRD patterns of (Ba,Ca)TiO₃ materials. (b) Magnified diagram of small angle range

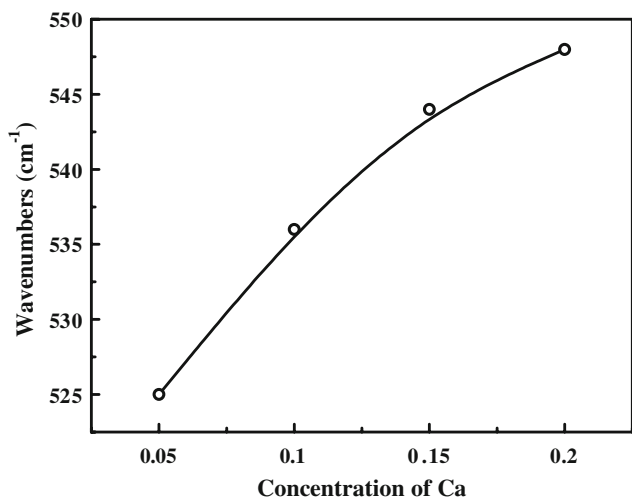


Fig. 6 Relationship between wavenumber of the absorption peak and the concentration of Ca in (Ba,Ca)TiO₃ materials

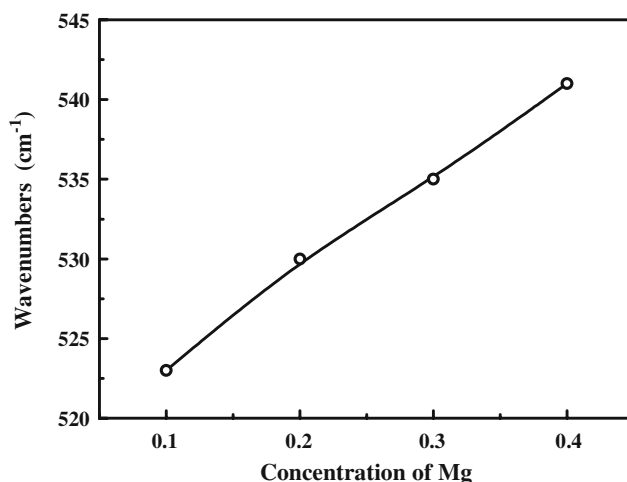


Fig. 8 Relationship between wavenumber of absorption peak and the concentration of Mg in (Ba,Mg)TiO₃ materials

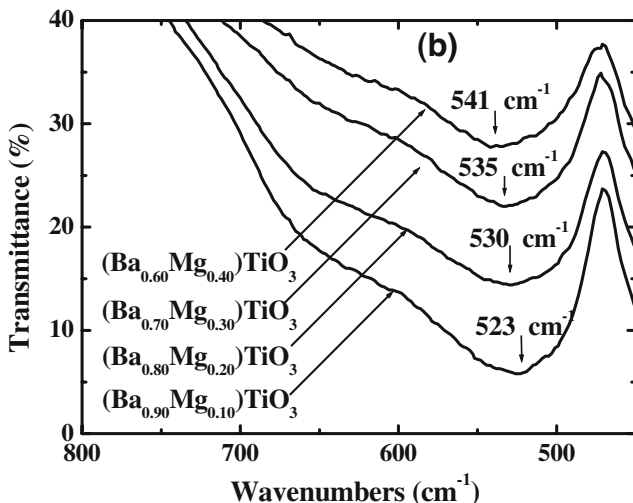
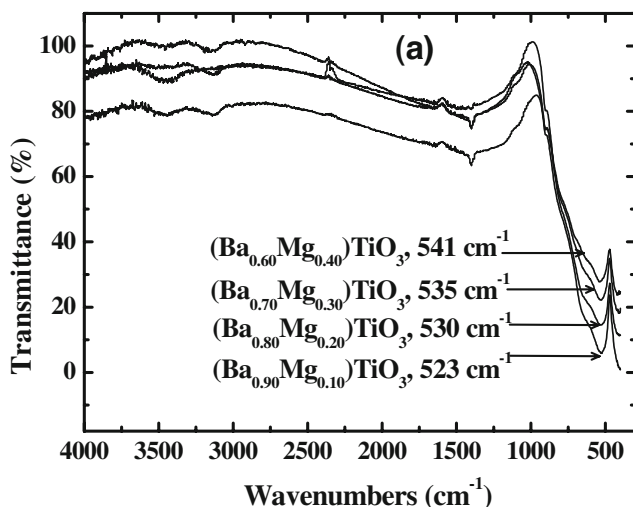


Fig. 7 (a) FTIR spectra of (Ba,Mg)TiO₃ materials. (b) Magnified diagram of absorption peak (the vertical position of some curve is adjusted to avoid overlap of curves)

FTIR measurement does not cover the region. The observed absorption frequency band, near 540 cm⁻¹, is assigned to the Ti–O₁ “stretching” normal vibration [Fig. (3b)]. This mode is very important because the direction of “stretching” normal vibration is along with that of spontaneous polarization in BaTiO₃ with tetragonal phase. So, it is mainly discussed in the paper. A further study about the other vibration modes will be carried out in future.

Figure 4 shows the FTIR spectra of BaTiO₃ doped with different concentration of Ca. It is obvious that the FTIR patterns of (Ba, Ca)TiO₃ and pure BaTiO₃ are similar. But, the wavenumber of absorption peak in (Ba_{0.95}Ca_{0.05})TiO₃ is smaller than that in the pure BaTiO₃. The former is 525 cm⁻¹ when the latter is 539 cm⁻¹. It is explained by the weakness of coulomb interaction. Figure (5a) shows that the (Ba,Ca)TiO₃ materials possess perovskite structure [18]. When Ca²⁺

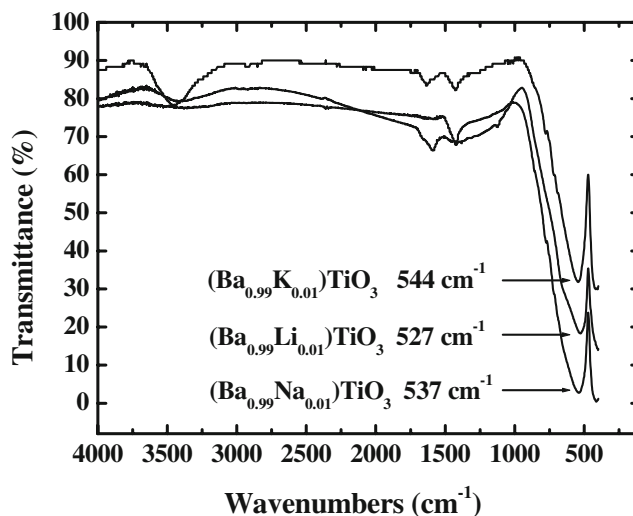


Fig. 9 FTIR spectra of BaTiO₃ material doped with Li, Na, and K (The vertical position of some curve is adjusted to avoid overlap of curves)

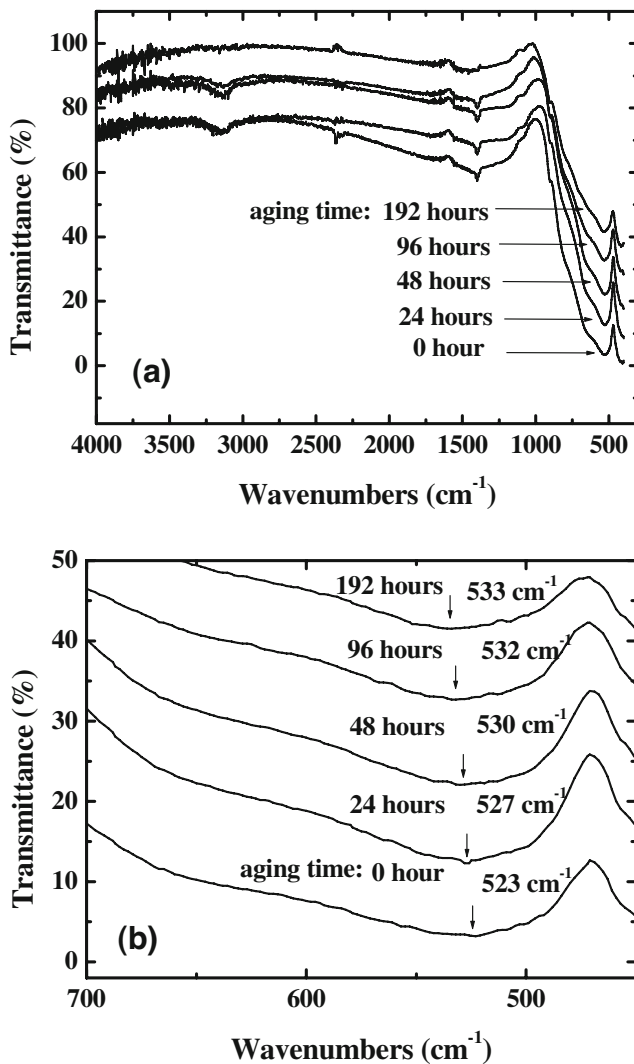


Fig. 10 (a) FTIR spectra of $(\text{Ba,Mg})\text{TiO}_3$ materials during aging at 50°C . (b) Magnified diagram of absorption peak (the vertical position of some curve is adjusted to avoid overlap of curves)

ions are doped, some of them enter B-site in the perovskite structure, even though most of them occupy A-site. The electric charge of Ca^{2+} is less than that of Ti^{4+} . Then, the coulomb force between Ca^{2+} and O^{2-} is weaker than that between Ti^{4+} and O^{2-} . It results in a decrease of energy of O–M (M=ion at B-site) bond. When the concentration of Ca increases, another effect exhibits. The wavenumber of the absorption peak increases with increase of the concentration of Ca. When Ca^{2+} ions are doped, most of them replace Ba^{2+} . The radius of Ca^{2+} is 0.099 nm, less than 0.133 nm of Ba^{2+} . So, the volume of the cell is decreased by doping. It is confirmed by the XRD patterns of $(\text{Ba,Ca})\text{TiO}_3$. Figure (5b) exhibits that the diffraction angle increases with increase of the amount of Ca, demonstrating that the distance between the crystal planes becomes shorter. Consequently, the force constant increases with contraction of the distance between Ti and O. Then, it can be observed that the absorption

wavenumber of Ti–O bond becomes larger with increase of the concentration of Ca (Fig. 6). The value of the wavenumber increases from 525 to 548 cm^{-1} when the concentration of Ca changes from 5 to 20 at. %.

The FTIR measurement of $(\text{Ba,Mg})\text{TiO}_3$ was carried out in order to testify if the effect is available in the parallel system. From Fig. 7, it is clear that the appearance is very similar. Two effects are included. First, the wavenumber of absorption peak in $(\text{Ba}_{0.90}\text{Mg}_{0.10})\text{TiO}_3$ is 523 cm^{-1} , smaller than 539 cm^{-1} of the pure BaTiO_3 . Second, the absorption wavenumber increases with the concentration of Mg. It changes from 523 to 541 cm^{-1} when the concentration of Mg changes from 10 to 40 at. % (Fig. 8). They are consistent with the phenomenon in $(\text{Ba,Ca})\text{TiO}_3$ very well, supporting the mechanism suggested above.

Furthermore, the effect of additives with hetero-valence is explored. Here, the FTIR spectra of BaTiO_3 doped with alkali are investigated (Fig. 9). Their chemical formulas are $(\text{Ba}_{0.99}\text{Li}_{0.01})\text{TiO}_3$, $(\text{Ba}_{0.99}\text{Na}_{0.01})\text{TiO}_3$, and $(\text{Ba}_{0.99}\text{K}_{0.01})\text{TiO}_3$, respectively. The absorption peak of the BaTiO_3 doped with K locates at 544 cm^{-1} . It is attributed to the change of lattice parameter. Because the radius of K^+ is smaller than that of Ba^{2+} , the cell parameter becomes smaller when K^+ replaces Ba^{2+} . The distance between Ti and O becomes shorter. The strength of Ti–O bond is enhanced. Then, a larger wavenumber of absorption peak is observed in the BaTiO_3 material doped with K. On the other hand, the mechanism is different when Li or Na is doped into the system. The wavenumbers of absorption peak become smaller, even though the radii of these two ions are smaller than that of K^+ . With consideration about the small size of Li^+ and Na^+ , some of them may enter B-site in perovskite ABO_3 of BaTiO_3 . This case is different from that of BaTiO_3 doped with K. Here, the effective electric charges of defects increase. One negative electric

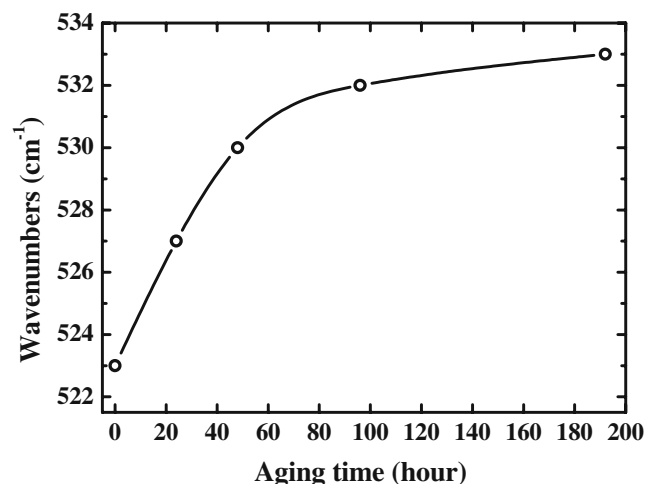


Fig. 11 Relationship between wavenumber of absorption peak and aging time in $(\text{Ba}_{0.90}\text{Mg}_{0.10})\text{TiO}_3$ material (aging temperature= 50°C)

charge is produced when a K^+ replaces a Ba^{2+} . Three negative electric charges are produced when a Li^+ (or Na^+) replaces a Ti^{4+} . To keep electric charge balance, the amount of O-vacancies in the latter is three times as large as that in the former. Therefore, Ti–O octahedrons are distorted or damaged more easily. The energy of lattice vibration becomes less because it is determined by the periodic structure of the crystal. This is why the $BaTiO_3$ doped with Li or Na exhibit relatively low absorption frequency. Comparing the radii of Li^+ , Na^+ , and Ti^{4+} , they are 0.06, 0.09, and 0.068 nm, respectively. It is clear that the radius of Li^+ is closer to that of Ti^{4+} . Therefore, Li^+ possesses a larger possibility to replace Ti^{4+} than Na^+ . Then, the effect in Li-doped sample is stronger. The wavenumber of absorption peak is the smallest among these three materials.

The aging effects of FTIR in $(Ba,Ca)TiO_3$ and $(Ba,Mg)TiO_3$ systems are observed. These two systems exhibit different behavior. The FTIR spectra of $(Ba,Ca)TiO_3$ are not changed significantly by aging. But, the FTIR curves of $(Ba,Mg)TiO_3$ are strongly affected by aging (Fig. 10). These results indicate that the FTIR spectra are determined not only by chemical compositions, but also by other factors. The structures of the two systems are very similar. But, the point defects in $(Ba,Mg)TiO_3$ are more than that in $(Ba,Ca)TiO_3$. The point defects are produced to keep electric charge balance. Mg^{2+} has a higher possibility to enter B-site than Ca^{2+} because the radius of Mg^{2+} is smaller than that of Ca^{2+} . It is close to the radius of Ti^{4+} at B-site as well. Because the chemical valences of Mg^{2+} and Ti^{4+} are different, the point defects must be induced. Point defects may diffuse to more stable positions during aging. Therefore, the FTIR spectra are changed by aging. The wavenumber of absorption peak shifts to a higher value when aging time is longer. From Fig. 11, it is observed that the wavenumber of $(Ba_{0.90}Mg_{0.10})TiO_3$ ceramics aged at $50^\circ C$ moves from 523 to 533 cm^{-1} when aging time changes from 0 hour (without aging) to 192 h. On the other hand, no significant variation of FTIR curve is observed in $(Ba,Ca)TiO_3$. Compare with the experimental results and structures in the two systems, the aging effect is attributed to the movement of point defects. It demonstrates that the FTIR spectrum is probably used to investigate the stability of the material and distribution of point defects.

4 Conclusion

The additives Ca, Mg, Li, Na and K are doped into $BaTiO_3$ ceramics. The FTIR spectra reveal that they affect the vibration of crystal lattices. When a smaller ion replaces Ba^{2+} , the cell becomes smaller, resulting in the distance between Ti and O becomes shorter. This enhances the interaction between these ions. The corresponding absorption

peak in FTIR spectrum shifts to a higher frequency with increase of the concentration of the additive. When an ion with less electric charge replaces Ti^{4+} , the coulomb interaction between O^{2-} and the cation in B-site is weakened. Then, the wavenumber of the corresponding absorption peak shifts to a lower frequency. When the radii of additives are very small, these ions have probability to occupy B-site and induce many O-vacancies. So, the ordinary structure of TiO_6 octahedron is distorted or damaged. The wavenumber of absorption peak decreases.

When the point defects exist, the FTIR spectra are affected by aging. The $(Ba,Ca)TiO_3$ possesses less point defects than the $(Ba,Mg)TiO_3$. The FTIR spectra of the latter are affected significantly by aging. On the contrast, the former exhibits a good stability during aging. The FTIR is a potential way to characterize the stability of this kind of functional materials.

Ferroelectricity and piezoelectricity in these systems are tightly related with the vibration of crystal lattices. Therefore, it is helpful to study some physical effect by means of the Fourier transformation infrared spectroscopy. A study about the correlation between phase transition, spontaneous polarization and FTIR in doped $BaTiO_3$ system is in progress.

Acknowledgement The authors would like to thank Shanghai Shuguang project (04SG48), Shanghai Leading Academic Discipline project (T0402), Shanghai Education Committee project (07ZZ66), and Shanghai Pujiang project (05PJ14082) for supporting the research.

References

1. K. Uchino, *Ferroelectric Device* (Dekker, New York, 2000), pp. 1–9
2. L.E. Cross, *Ferroelectrics* **151**, 305 (1994)
3. D. Sun, M. Zhao, H. Luo, Z. Yin, J. Inorg. Mater. **15**, 939 (2000)
4. D. Sun, X. Ren, K. Ostuka, *Appl. Phys. Lett.* **87**, 142903 (2005)
5. Y. Xu, *Ferroelectric Materials and Their Applications* (Elsevier Science Publisher B. V., Amsterdam, 1991), pp. 129–142
6. B. Noheda, N. Duan, N. Cereceda, J.A. Gonzalo, J. Korean Phys. Soc. **32**, S256 (1998)
7. D. Sun, S. Lin, J. Korean Phys. Soc. **32**, S205 (1998)
8. P. Qiu, W. Luo, A. Ding, J. Inorg. Mater. **16**, 928 (2001)
9. R.B. Atkin, R.M. Fulrath, J. Am. Ceram. Soc. **54**, 313 (1971)
10. P. Qiu, A. Ding, X. He, W. Luo, *Proc SPIE* **4086**, 692 (2000)
11. K. Babooram, Z.G. Ye, *Chem. Mater.* **16**, 5365 (2004)
12. F.X. Perrin, V. Nguyen, J.L. Vernet, *J. Sol–Gel Sci. Tech.* **28**, 205 (2003)
13. R. Asiaie, W. Zhu, S.A. Akbar, P.K. Dutta, *Chem. Mater.* **8**, 226 (1996)
14. K. Nomura, Z. Homonnay, G. Juhasz, A. Vertes, H. Donen, T. Sawada, *Hyperfine Interact* **139**, 297 (2002)
15. S.K. Lee, S.S. Ryu, D.H. Yoon, *J. Electroceram.* **18**, 1 (2007)
16. C.H. Perry, B.N. Khanna, *Phys. Rev.* **105**, A408 (1957)
17. J.T. Last, *Phys. Rev.* **105**, 1740 (1957)
18. JCPDS Powder Diffraction File Card No. 05–526, International Centre for Diffraction Data, Newtown Square, PA, 1967